Geological Society of Malaysia, Bulletin 46
May 2003; pp. 231–238

Fluid inclusions studies of Bukit Botak skarn deposit, Mengapor, Pahang

GOH SWEE HENG[1], TEH GUAN HOE[2] AND MOHD ROZI UMOR[1]

[1]Program Geologi, PPSSSA, Fakulti Sains dan Teknologi
43600 UKM Bangi, Selangor
Universiti Kebangsaan Malaysia
[2]Department of Geology, University of Malaya
50603 Kuala Lumpur

Abstract: The lithology of Mengapor area consists of Permian limestone, volcanic, metasediment as well as Triassic granodiorite. Bukit Botak comprises of at least 300 m of rhyolitic tuff at the upper part and adamellite intrusive at the lower portion. Four quartz veins samples from different levels of borehole M15 and M33A at Zone A (Cu-Au in skarn) were selected for fluid inclusion study. Fluid inclusion study indicated that the homogeneous temperature for M15 and M33A is ranging from 219.4°C to 313.7°C and 169.2°C to 221.4°C respectively. While the freezing point for M15 vary from -5.1°C to -1.4°C, giving the paleodepth from 232 m to 1,152 m. These inclusions are generally of low salinity (2.42 to 8.02 wt% NaCl equivalent), with a median salinity value of 5.0 wt% NaCl. However, the paleodepth for M33A is relatively shallow ranges from 52 m to 237 m with freezing point of -5.1°C to -2.2°C, the salinity in these inclusions is slightly higher than M15, recorded as 3.72 to 8.02 wt% NaCl. Result from Haas diagram also indicated that the trapping pressure for M15 is ranging from 22 to 98 bars, while M33A recorded as 6 to 23 bars. The homogeneous temperatures and salinities data suggest that the sources of fluids in quartz vein of borehole M15 (level 215 m) and M33A (level 166 m and 284 m) are probably the same. The salinity of fluid inclusion M15 at level 352 m is basically lower than 3.08 equiv. wt% NaCl, suggested to be meteoric origin. The overall salinity of inclusions in quartz samples is ranging from as low as 2.42 to 8.02 equiv. wt% NaCl, while the homogeneous temperatures range from 169.2 to 313.7°C indicated that this is a retrograde quartz in gold skarn formed during last stage of skarn evolution. Fluid inclusions study also suggested the Mengapor deposit as distal skarn which is located at relatively shallow depth, low salinity and low temperatures.

INTRODUCTION

The Mengapor deposit, located about 20 km northeast of the town of Maran (Fig. 1) was discovered by Geological Survey of Malaysia during the survey of regional geochemistry of north Pahang. Mengapor deposit was recognized as anomaly 8108 with 150 km^2. This is a multi-element Pb-Zn-Cu-Mo-Sn anomaly with subordinate anomalies for Fe, W and As by several gold mineralization surveys at northern Pahang as well as Mengapor area, Mengapor deposit has recently recognized as gold bearing skarn in eastern gold belt. An extensive programmes of pitting and diamond drilling were carried out by Malaysia Mining Corporation Berhad (MMC) in 1983. During the year of 1986, 1990 and 1993, geochemical and mineralogical studies on Mengapor Deposit were carried out by Geological Survey of Malaysia (Gunn *et al.*, 1993).

According to prospective gold areas in the Regional Mineral Exploration Project Report produced by Geological Survey of Malaysia (Lee, *et al.*, 1986), a high prospect anomaly has been located at the immediate surrounding of Bukit Botak. MMC has divided the mineralization at this area into three mineralization zones. Zone A, located at south-eastern part of Bukit Botak, relatively enriched in Cu and Au in sulphides ores of skarn and vein type. Zone B is located at the south-west of the rhyolitic tuff, consists

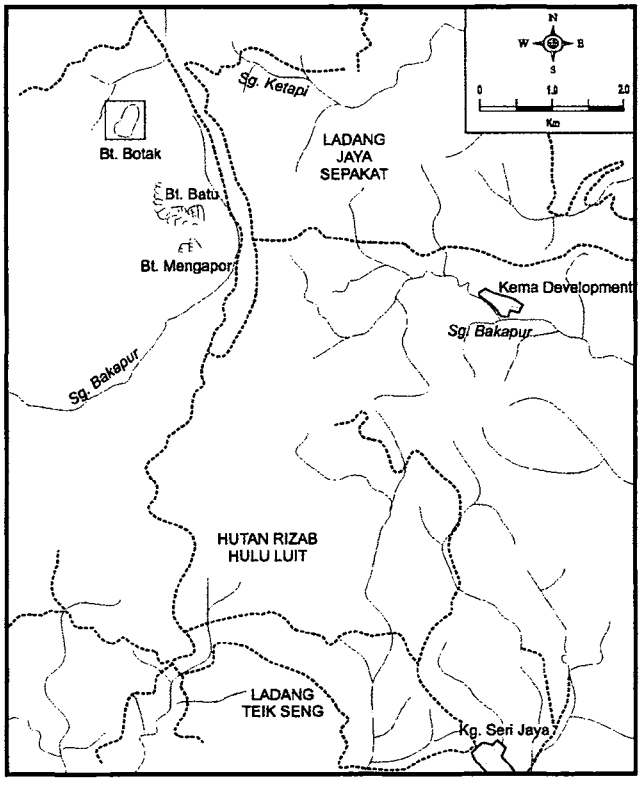

Figure 1. The location map of the study area at Bukit Botak, Mengapor deposit, Pahang.

mainly of sulphides ores of skarn with enrichment in Cu and Ag. While Zone C located at the northern part of Bukit Botak and mainly comprises of thick layer gossanous oxide ore zone, with enrichment of Cu as well as Ag. The occurrence of gold in Zone B and Zone C are relatively rare compare to Zone A, however, the average gold grade in the latter zone is generally less than 0.5 ppm.

The purpose of this research is to carry out fluid inclusion studies for quartz veins in Zone A in order to improve the gold mineralization information in this zone. Both selected boreholes are located within Zone A at the south-eastern part of Bukit Botak.

GEOLOGY OF THE MENGAPOR DEPOSIT

The Mengapor deposit is underlain by thick layer of Permian sedimentary rocks deposited in a shallow basin environment. The late Permian volcanics and Lower Triassic adamellite have extruded into these sediments. At the periphery of Bukit Botak, the sedimentary rocks (Seri Jaya beds) were metamorphosed to skarns with minerals of predominated by diopside and garnet. Bukit Botak (592 m) itself comprises of rhyolitic tuff at the upper part and adamellite intrusive at the lower portion. Rhyolitic tuff and tuff breccia show silicification and limonitization, but sulfide minerals are rarely recognized. Whilst the adamellite intrusive is commonly fractured with fine hydrothermal veins containing sulphides. The dark grey to ochre-coloured rhyollitic tuff is consisting mainly of fine to medium grained pyroclastic and fragments of sedimentary rocks. Angular to subangular quartz grains are easily observed in hand specimen, while flakes of chlorite and grains of fine quartz aggregates are enclosed in quartz sericite matrix. The thickness of Bukit Botak tuff obtained from diamond drilling indicated to be at least 300 m (Lee and Chand, 1981).

The Seri Jaya beds consist of two facies: the calcareous Mengapor limestone and older argillaceous facies, predominated by slate. The Mengapor limestone consists primarily of grey, massively bedded and strongly jointed marble with lesser calcareous graphitic slate, graphitic and non-graphitic phyllite and schist. The slate consists mainly of pelitic hornfels, graphitic slate and quartz-sericite phyllite. Subordinate interbeds of quartzite, schist, non-carbonaceous slate and argillite also occur. Minor interbeds of metatuff, metasiltstone, calc-silicates and slightly metamorphosed sandstone are present (Lee, 1990). Figure 2 shows the geological map of Bukit Botak and its immediate surrounding area, while Figure 3 and Figure 4 show the schematic cross section of the study area.

PETROGRAPHY AND ORE MINERALOGY

The country rocks at the immediate surrounding area of Bukit Botak are mainly consisting of carbonaceous limestone interbeded with calcareous shale. Initial isochemical metamorphism has recrystallize the limestone to marble, shales to hornfels and sandstones to quartzites. The infiltration of the contact rocks by hydrothermal fluids leads to the conversion of these early metamorphic rocks to skarn with minerals predominated by diopside and garnet. Wollastonite, tremolite-actinolite, epidote, sericite, chlorite, vesuvianite and altered feldspar are present in minor amounts. Calcite is widespread in the skarn, observed as either associated with diopsite or occurs in vein form which normally occupy the inner part of the quartz vein. Two types of quartz veins can be observed in this skarn, the coarse grain quartz and the relatively fine grain quartz that occurred together with calcite vein. The metallic mineralization is normally present in the latter quartz vein; while the former is usually devoid of any minerals.

The major minerals present in the ore sample from borehole M33A and M15 are pyrrhotite, chalcopyrite and sphalerite. Pyrite, magnetite, arsenophyrite, marcasite, galena, bismuth, tellurides and covellite are present in relatively low amount. However, free gold grains have not been observed in the ore samples.

FLUID INCLUSION STUDIES

There are different types of quartz and quartz-calcite veins within the skarn deposit, and not all are associated with gold mineralization. Detailed study of core samples reveals at least three types of veins: (1) laminated quartz veins, with lamina thickness varying from a few millimeters to a few centimeters, (2) smoky quartz veins, and (3) some late quartz-calcite veins. Among these, only the laminated quartz veins, which account for the bulk of gold mineralization were used for fluid inclusion studies. Samples collected from two different boreholes (M33A and M15) at different levels. Figure 4 shows the location of the boreholes as well as levels of quartz samples collected.

Three different types of inclusions, based on their spatial variations, were identified. These are: type I inclusions, occurring randomly and in isolation within quartz porphyroclasts (size = 3-26 μm), interpreted to be the primary inclusions related to the formation of the quartz veins and associated gold precipitation (Fig. 5 and Fig. 7); type II inclusions or pseudosecondary inclusions (size = 1 - 13 μm), occurring along healed micro-fractures within the porphyroclasts; interpreted as syngenetic microcracks healed during crystal growth (Fig. 7), type III inclusions (size < 3 μm) arranged along the grain boundaries or sub-grain boundaries, and interpreted as epigenetic fractures, have been trapped during grain boundary migration or dynamic recrystallization processes, secondary in nature and representing the youngest inclusion type (Fig. 6 and Fig. 8). Textural relationships, distribution and characteristics of the different types of the fluid inclusions are also briefly described as follows.

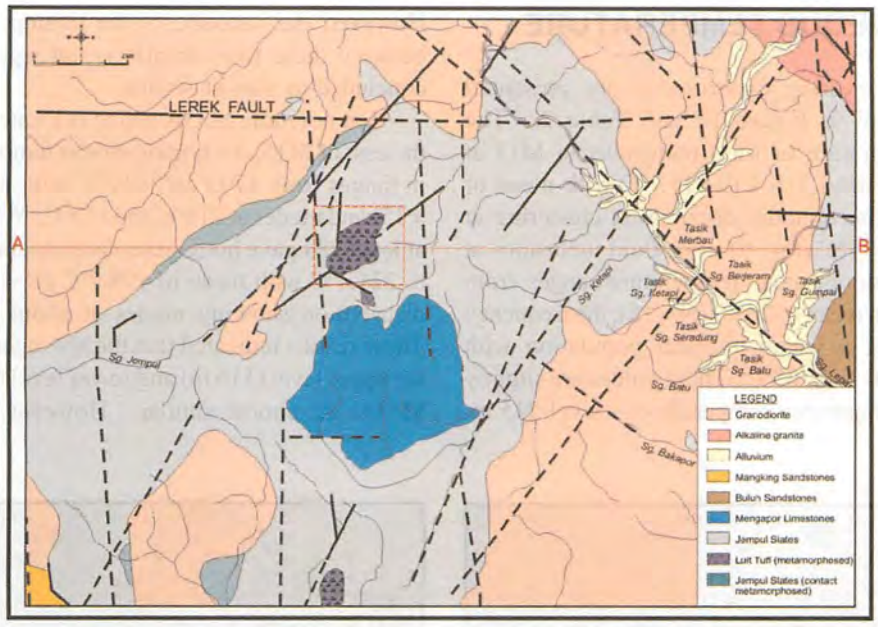

Figure 2. Location and geological map of study area at Bukit Botak, Mengapor deposit, Pahang.

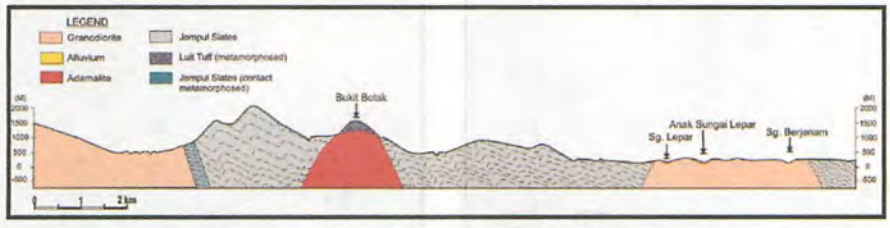

Figure 3. Geological section across of the Bukit Botak (A-B, refer Fig. 2), Mengapor deposit.

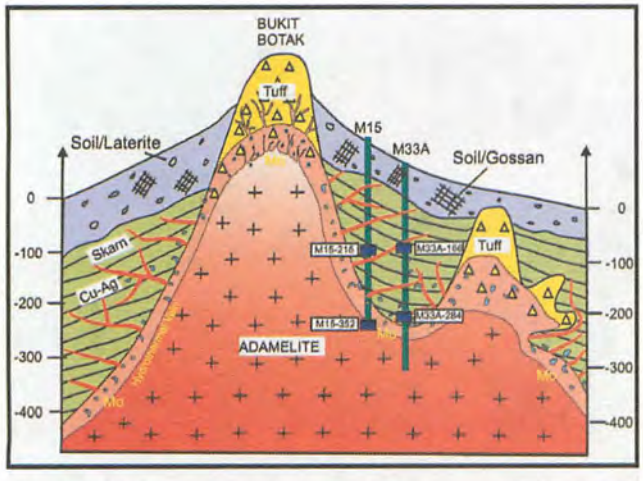

Figure 4. Schematic geological section across Bukit Botak, Mengapor deposit (modified after Gunn, *et al.*, 1993)

ANALYTICAL PROCEDURES OF MICROTHERMOMETRY

Microthermometric measurements were carried out on fluid inclusion in four doubly-polished sections from Mengapor deposit. Two samples were collected from borehole M33A at 166 m and 284 m depth, another two from borehole M15 at 215 m and 352 m. Work was done using a gas flow, dual purpose Linkam heating and freezing stage at Indonesian Institute of Science (LIPI), Indonesia, following the procedures outlined by Roedder (1984) and Shepherd *et al.* (1985).

Routinely available measurements are homogenization temperatures and final melting temperatures. The measurements were made by placing an inclusion-bearing sample in an enclosed heating-cooling cell under a microscope and observing phase changes by eye. This permits a measurement precision of ±0.1°C and an accuracy, after calibration, of within ±1.0°C. In addition, first melting (eutectic) temperatures can sometimes be estimated for larger inclusions, but the measurement is less precise, rarely better than ±5°C.

The summary of fluid inclusion data are as shown in Table 2. Freezing and heating experiments were also restricted to the primary fluid inclusions of Types I–II.

HOMOGENEOUS TEMPERATURE

Results of the heating experiments are presented graphically in Figure 9, Figure 10 and Table 2. The homogeneous temperature of fluid inclusions in M15 at level 215 m ranges from 219.4 to 313.7°C with mean of 273.6°C (N = 15), the bimodal distribution clustering at around 265°C and 305°C (Fig. 9). For fluid inclusions at level 352 m, the homogeneous temperature ranges from 220.4 to 293.4°C with mean of 265.0 (N = 15), the frequency distribution showing a vague bimodal population with modes at about 265°C and 285°C. These values are slightly lower than the homogeneous temperature at level 215 m. However, the variance of the homogeneous temperature between these two samples is not significant and can be concluded as almost similar.

For borehole M33A which is located at about 200 m to the east of M15, the homogeneous temperature at level 166 m ranges from 170.1 to 214.3°C with mean of 191.1°C (N = 15) and modes at 215°C and 175°C. While fluid inclusions at level 284 gave homogeneous temperature range of 169.2 to 221.4°C with mean of 198.7°C (N = 15), the frequency distribution showing modes at about 225°C and 175°C. These results indicated that the homogeneous temperatures for upper level (116 m) and lower level (284 m) of borehole M33A are almost similar. However, the homogeneous

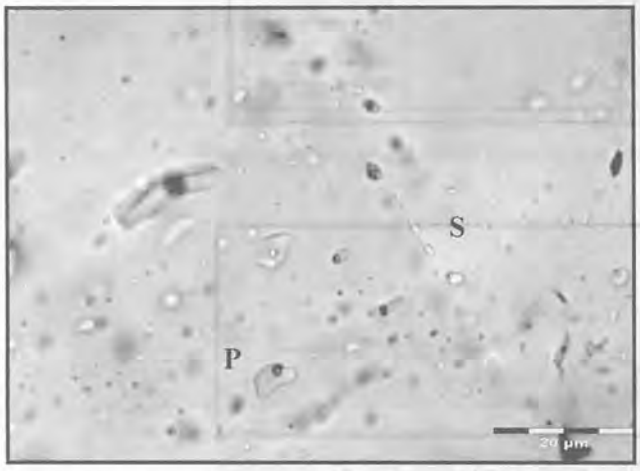

Figure 5. Primary inclusions with small vapor (10 to 15%) grow in quartz crystal. While the secondary inclusions occur as planar groups, outlining healed fractures and are thin, flat or irregular in shape, samples from borehole M15 at 352 m.

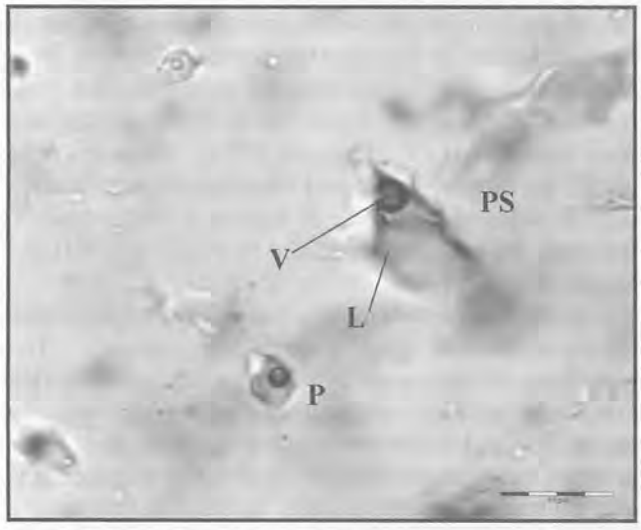

Figure 7. Primary inclusions (P) form in growing quartz crystal and the pseudo-secondary inclusions (PS) fill the overlap, the host crystal was fractured essentially as the crystal was growing. Most of the fluid inclusions in M33A-166 are consist of two phases inclusions, liquid (L) with small vapor (V) of 15 to 20%, however daughter minerals are fairly exist, sample from borehole M33A at 166 m.

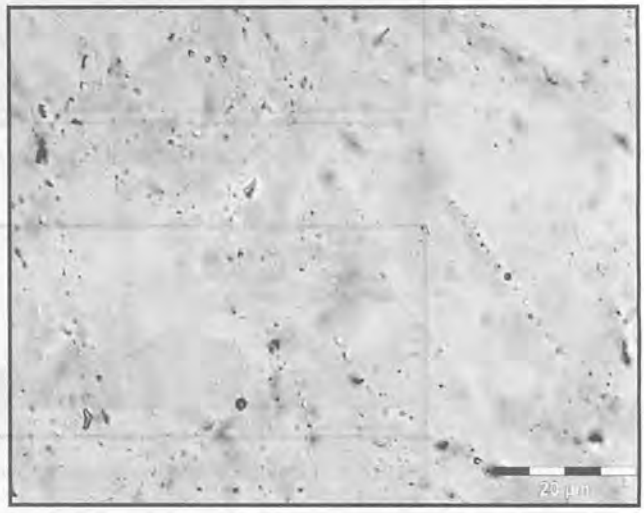

Figure 6. Secondary fluid inclusions arranged as planar groups along grain boundaries or sub-grain boundaries which is interpreted as epigenetic fractures, have been trapped during recrystallization process, sample from M15 at 352 m.

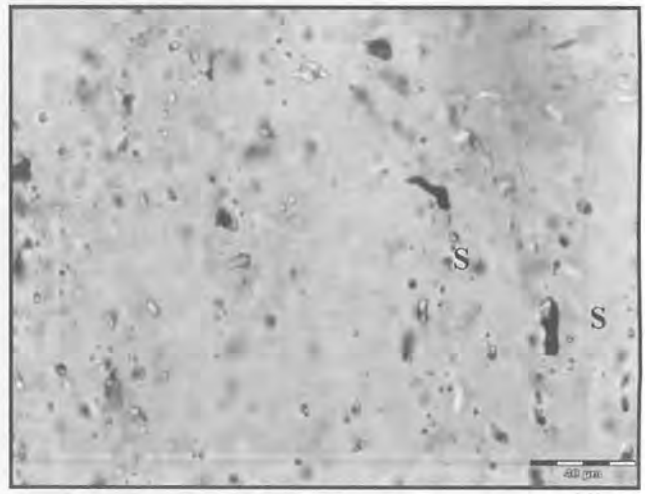

Figure 8. Secondary fluid inclusions (S) arranged along the grain boundaries or sub-grain boundaries which is interpreted as epigenetic fractures, have been trapped during recrystallization process, sample from borehole M33A at 166 m.

Table 1. Microthermometry data for fluid inclusions from the Bukit Botak, Mengapor deposit.

Host Mineral	FI No.	Void		Bubble	Micro thermometry		Remarks	Host Mineral	FI No.	Void		Bubble	Micro thermometry		Remarks
		W(μm)	L(μm)	ø(μm)	Tm(°C)	Th(°C)				W(μm)	L(μm)	ø(μm)	Tm(°C)	Th(°C)	
Mengapor (M15-215)								**Mengapor (M33A-166)**							
Quartz	01	4.2	4.9	1.2	-5.1	313.7	Primary, anhedron	Quartz	01	5.4	5.8	1.2	-5.1	214.3	Primary, anhedron
Quartz	02	4.2	4.8	1.2	-4.6	303.4	Primary, anhedron	Quartz	02	3.6	4.6	1.1	-4.6	214.3	Primary, subhedron
Quartz	03	5.4	12.8	1.4	-5.1	303.4	Primary, necking	Quartz	03	3.6	4.2	1.1	-4.2	199.2	Primary, anhedron
Quartz	04	5.2	5.8	1.8	-3.6	260.2	Primary, euhedron	Quartz	04	10.2	14.8	1.4	-3.8	170.1	Primary, anhedron
Quartz	05	4.4	6.6	1.4	-2.7	219.4	Primary, anhedron	Quartz	05	4.4	10.8	1.4	-2.7	159.2	Primary, necking
Quartz	06	3.6	10.8	1.2	-3.6	260.2	Primary, necking	Quartz	06	3.4	9.8	1.1	-2.7	159.2	Primary, necking
Quartz	07	3.2	5.2	1.0	-4.6	303.4	Primary, anhedron	Quartz	07	13.8	15.2	1.1	-4.2	199.2	Primary, anhedron
Quartz	08	4.4	6.4	1.2	-4.6	303.4	Primary, anhedron	Quartz	08	4.8	6.4	1.2	-4.2	199.2	Primary, anhedron
Quartz	09	4.3	4.9	1.2	-3.6	260.2	Primary, euhedron	Quartz	09	5.6	8.4	1.8	-4.6	199.2	Primary, anhedron
Quartz	10	4.6	4.8	1.3	-3.6	260.2	Primary, anhedron	Quartz	10	3.4	5.2	1.1	-4.6	214.3	Primary, anhedron
Quartz	11	5.1	8.4	1.6	-5.1	313.7	Primary, anhedron	Quartz	11	4.5	5.6	1.2	-3.8	170.1	Primary, subhedron
Quartz	12	5.4	8.6	1.6	-2.7	219.4	Primary, subhedron	Quartz	12	4.2	4.9	1.1	-4.2	214.3	Primary, anhedron
Quartz	13	4.2	6.6	1.2	-3.6	260.2	Primary, anhedron	Quartz	13	5.2	8.4	2.1	-3.8	170.1	Primary, anhedron
Quartz	14	3.8	6.7	1.1	-4.6	303.4	Primary, anhedron	Quartz	14	5.4	8.4	2.1	-4.2	214.3	Primary, anhedron
Quartz	15	4.8	12.4	1.8	-3.6	219.4	Primary, necking	Quartz	15	3.8	8.4	1.0	-2.7	170.1	Primary, necking
Mean					**-4.0**	**273.6**		**Mean**					**-4.0**	**191.1**	
Mengapor (M15-352)								**Mengapor (M33A-284)**							
Quartz	01	18.6	25.5	7.8	-1.6	280.2	Primary, anhedron	Quartz	01	10.8	15.4	1.2	-4.6	221.4	Primary, subhedron
Quartz	02	16.6	24.4	7.2	-1.6	280.2	Primary, anhedron	Quartz	02	6.4	8.4	2.1	-4.6	221.4	Primary, anhedron
Quartz	03	4.8	8.3	1.4	-1.6	280.2	Primary, subhedron	Quartz	03	3.4	8.4	1.6	-2.8	178.8	Primary, necking
Quartz	04	3.6	8.5	1.2	-1.4	268.3	Primary, anhedron	Quartz	04	8.4	14.6	1.0	-2.2	169.2	Primary, anhedron
Quartz	05	3.8	6.4	1.1	-1.4	268.3	Primary, anhedron	Quartz	05	4.2	6.4	1.2	-4.0	199.6	Primary, anhedron
Quartz	06	5.4	8.4	1.4	-1.8	293.4	Primary, anhedron	Quartz	06	4.1	6.7	1.1	-4.0	199.6	Primary, anhedron
Quartz	07	5.4	8.6	11.2	-1.4	248.8	Primary, anhedron	Quartz	07	3.8	6.2	1.0	-4.6	21.4	Primary, anhedron
Quartz	08	5.2	10.6	1.2	-1.6	220.4	Primary, subhedron	Quartz	08	8.6	14.8	1.0	-3.4	178.8	Primary, anhedron
Quartz	09	4.3	12.4	1.4	-1.8	268.3	Primary, necking	Quartz	09	4.5	6.4	1.1	-3.4	178.8	Primary, anhedron
Quartz	10	4.6	4.8	1.4	-1.6	268.3	Primary, anhedron	Quartz	10	5.4	8.4	1.4	-4.6	221.4	Primary, anhedron
Quartz	11	3.8	4.9	1.1	-1.4	248.8	Primary, anhedron	Quartz	11	5.6	6.8	1.6	-4.6	221.4	Primary, anhedron
Quartz	12	5.4	10.2	2.1	-1.6	220.4	Primary, subhedron	Quartz	12	3.7	8.2	1.0	-2.2	169.2	Primary, anhedron
Quartz	13	5.6	9.4	2.0	-1.8	268.3	Primary, subhedron	Quartz	13	4.5	8.6	1.1	-2.8	199.6	Primary, anhedron
Quartz	14	6.7	8.4	2.4	-1.8	293.4	Primary, anhedron	Quartz	14	4.4	8.9	1.1	-3.4	178.8	Primary, necking
Quartz	15	6.8	7.4	2.1	-1.8	268.3	Primary, anhedron	Quartz	15	4.1	4.6	1.1	-4.6	221.4	Primary, anhedron
Mean					**-1.6**	**265.0**		**Mean**					**-3.7**	**198.7**	
Explanation of Abbreviations: W = Width, L = Length; Ø = Diameter															

Table 2. The summary of the interpretation data for fluid inclusions from Bukit Botak. Mengapor deposit.

Name of Sample	Homogeneous Temperature (Th) °C	Ice Melting Temperature (Tm) °C	Salinity Eq wt% NaCl	Paleo-depth (m)	Trapping Pressure (bar)
M15-215	219.4 – 313.7	-5.1 – -2.7	4.50 – 8.02	232 – 1,152	22 – 98
M15-352	220.4 – 293.4	-1.8 – -1.4	2.42 – 3.08	248 – 930	23 – 77
M33A-166	170.1 – 214.3	-5.1 – -2.7	4.50 – 8.02	52 – 206	6 – 20
M33A-284	169.2 – 221.4	-4.6 – -2.2	3.72 – 7.32	71 – 237	8 – 23

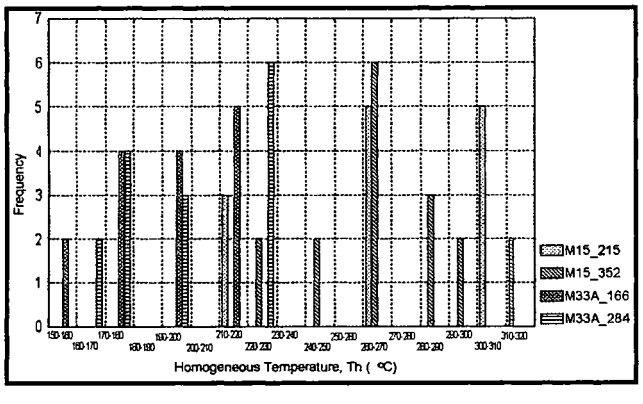

Figure 9. Histogram of homogeneous temperatures for fluid inclusions from the Bukit Botak, Mengapor deposit.

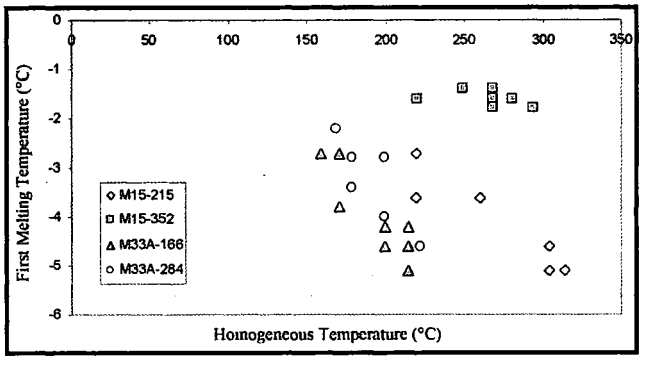

Figure 10. Plot of homogeneous temperatures vs first melting temperatures for fluid inclusions from Bukit Botak, Mengapor deposit.

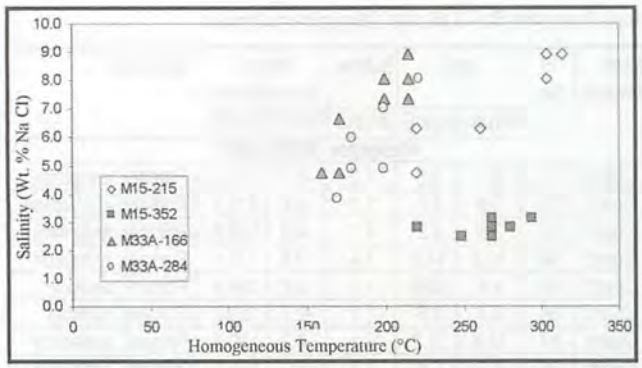

Figure 12. Plot of homogeneous temperatures vs salinity for fluid inclusions from Bukit Botak, Mengapor deposit.

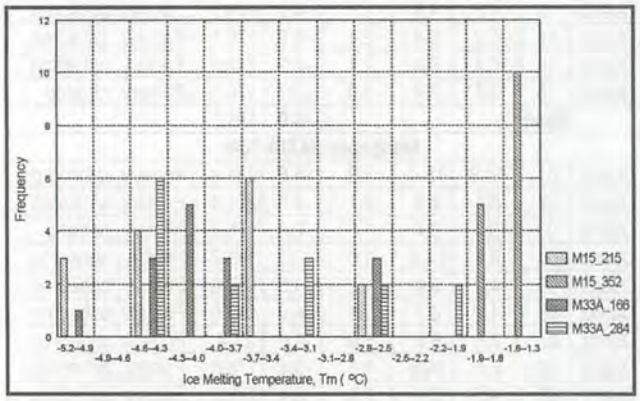

Figure 11. Histogram of first melting temperatures for fluid inclusions from the Bukit Botak, Mengapor deposit.

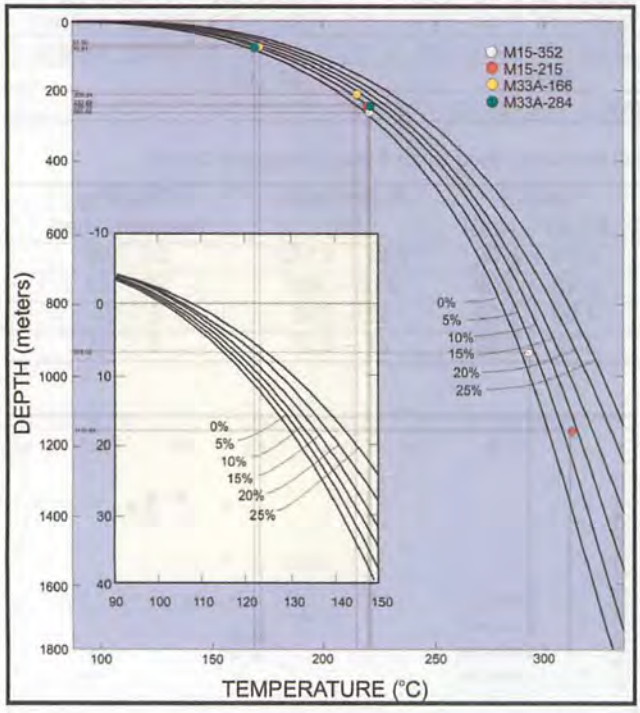

Figure 13. Boiling point vs depth curves for pure water (H_2O) and for brine of constant composition given in percent NaCl (Hass, 1971). The homogeneous temperatures (170.1°C to 313.7°C) of the Mengapor fluid inclusions at a depth of 52 m to 1,152 m below the surface.

temperature in borehole M33A is basically lower than borehole M15. The variation of homogeneous temperature for the quartz samples between these two boreholes is significant, ranges from 33 to 43%.

FREEZING TEMPERATURE

Freezing temperature data consisted of first melting point, freezing point depression and melting of clathrate, only first melting point measurements could be obtained from microthermometry study. The first melting points for fluid inclusions in borehole M15 at level 215 m range from -5.1°C to -2.7°C with mean of -4.0°C, the frequency distribution showing a vague bimodal population with modes at about -3.6°C and -4.5°C. Nevertheless, the temperature of first melting point at level 352 m is relatively high compare to level 215 m, these data show a small variation from -1.8°C to -1.4°C with mean of -1.6°C, modes at -1.5°C and -1.8°C (Fig. 11, Tables 1 and 2).

The first melting points for inclusions in M33A at level 166 m and 284 m are almost similar, range from -5.1°C to -2.7°C and -4.6°C to -2.2°C respectively. The mean value for 166 m is -4.0°C and modes on -4.2°C and -3.8°C, while first melting point at level 284 m recorded mean of -3.7°C and modes at -4.5°C and -3.3°C. These values are almost similar with the data from borehole M15, level 215 m. The first melting point temperatures of down to -5.1°C suggest that the skarn fluids may contain salts other than that of sodium (e.g. calcium and magnesium).

SALINITY

The calculated salinity values are presented as plot in Figure 12 and show a small variation from 2.42 to 8.02 equiv. wt% NaCl. Details of salinities for fluid inclusions in individual quartz samples are given in Table 2.

The salinities of the inclusions from borehole M15 at level 215 m range from 4.50 to 8.02 equiv. wt% NaCl, represented by few measurements (N = 15). Fifteen analyses from level 352 m gave relatively low salinity ranges from 2.43 to 3.08 equiv. wt% NaCl. The inclusions at M33A showed low salinities of 4.50 to 8.02 equiv. wt% NaCl for level 166 m and 3.72 to 7.32 equiv. wt% NaCl for level 284 m.

Figure 12 is a scatter plot showing the relationship between homogenization temperature and salinity data for borehole M15 and M33A of Mengapor skarn deposit. There appears to be a permissible relationship between homogenization temperature and salinity. The temperature and salinity data suggest that the sources of fluids in the borehole M15 (level 215 m) and M33A (level 166 m and 284 m) are probably the same. The salinity of fluid inclusion at M15 level 352 is basically lower than 3.08 equiv. wt% NaCl, suggested to be meteoric origin. The salinity for all samples from both boreholes range from as low as 2.42 to 8.02 equiv. wt% NaCl, these result is similar with data summarized in Meinert (1993), who concluded that the

retrograde quartz in gold skarn have homogeneous temperatures of 290 to 380 °C and salinity of 2.5 to 10.5 equiv. wt% NaCl.

PALEO-DEPTH

The homogeneous temperature and salinity of the inclusions are used to determine the paleo-depth of the inclusions. The paleo-depth for borehole M15 ranges from 232 to 1,152 m. However, inclusions at M33A indicated relatively low paleo-depth, range from 52 to 237 m.

THERMOBAROMETRY

Estimation of P-T has been attempted by the method of intersecting isochores of coexisting carbonic and aqueous biphase inclusions (Roedder and Bodnar, 1980). Isochores of the aqueous and carbonic inclusions are plotted on a P-T diagram. The trapping pressure for inclusions at M15 indicated wide variation, ranges 22 to 98 bars. While the trapping pressure at M33A are relatively low compare to M15, recorded as low as 6 to 23 bars.

SKARN METASOMATIC EVOLUTION

On the whole, the metasomatic evolution of the skarn agrees with the model of Evans (1993). At the beginning of the process, isochemical thermal metamorphism would have caused the marble and hornfels currently bordering the skarn to form. The earliest and most widespread mineral in the skarn is garnet. The principal process involved in this early stage is diffusion of elements in what can be an essentially stationary fluid, apart from the driving out of some metamorphic water.

During the second metasomatic stage, the pyroxene replaces garnet. Its composition varies with time from fine crystalline diopside, which replaces garnets, to coarser crystalline hedenbergite, which mainly occurs in veins and fractures. The infiltration of the contact rocks by hydrothermal fluids leads to the prograde metamorphic and metasomatic process operating at temperatures of about 400 to 800°C (Kwak and Tan, 1981) during which an ore fluid evolves, initial ore deposition takes place and the intrusion body begins to cool. Deposition of oxides and sulphides commences late in this stage but generally peaks during the third stage.

The third stage is a retrograde stage accompanying cooling of the associated pluton and involving the hydrous alteration early skarn minerals and parts of the intrusion by circulating meteoric water. Declining temperatures lead to the formation of sulphides minerals as well as gold in Mengapor deposit.

During the first hydrothermal stage, which took place at high temperature (>400°C), gold was probably transported as a chloride complex and precipitated as a result of unmixing phenomena due to cooling (Cameron and Hattori, 1987). The last hydrothermal stage is produced along fractures and faults affecting both the intrusion body and the skarn and caused chloritization of garnet and pyroxene, and sericitization of feldspar. It is characterized by the association of quartz, calcite, phyrrotite, chalcopyrite, sphalerite, and small amounts of arsenopyrite, molybdenite, pyrite, and stannite. During this hydrothermal stage, at lower temperature (<400°C), the fluid inclusions are of low salinity, aqueous and carbonic. In this case, gold probably was transported as a bisulfide complex and deposited either by loss of sulfur, which separated as sulfides, or by loss of H_2S by boiling.

Fluid inclusion data agree with the model of this evolution, with gradual cooling of the system, indicated by relatively high homogeneous temperatures at M15 (219.4 to 313.7°C) and low homogeneous temperature at M33A (169.2 to 221.4°C). However, the overall homogeneous temperatures at 169.2 to 313.7°C suggested that the development of first and second stages of skarn evolution are not significant, this deposit also can be interpreted as distal skarn deposit which was located at relatively shallow depth (52 to 1,152 m). Conversely retrograde alteration during cooling (last stage) and the possible influx of meteoric water will be probably be more intense at shallow rather than at deeper levels.

CONCLUSIONS

The fluid inclusions study of Mengapor deposit indicated that this is a distal skarn type deposit, with relatively shallow depth (52 to 1,152 m) and low salinities (2.42 to 8.02 equiv. wt% NaCl. The homogeneous temperatures of fluid inclusions range from 169.2 to 313.7°C, which is almost similar with the suggested temperatures of 210 to 350°C by Kwak and Tan (1981) for distal skarn. The trapping pressures obtained from the P-T diagram varies from as low as 6 to 98 bars.

ACKNOWLEDGEMENTS

This research was part of a post graduate study by the author at Geology Department, University of Malaya, financially supported by grant from the Project IRPA 02-02-02-0020. We wish to acknowledge Dr. Yeap Ee Beng and Dr. Wan Fuad Wan Hassan for their advice and support on this research.

REFERENCES

CAMERON, E.I. AND HATTORI, K., 1987. Archean gold mineralization and oxidized hydrothermal fluids. *Econ. Geol. 82*, 1177-1191.

EVANS, A.M., 1993. *Ore Geology and Industrial Minerals: An Introduction*. Blackwell Science Inc.

GUNN, A.G., PAUL, P.S. AND ZULKIPLI, C.K., 1993. Geochemical and mineralogical studies of gold in the Mengapor deposit, Pahang, Malaysia. *Geological Survey of Malaysia, Gold sub-programme Report 93/4*, 43p.

HAAS JR., J.L., 1971. The effect of salinity on the maximum thermal

gradient of a hydrothermal system at hydrostatic pressure. *Econ Geol. 66*, 940–946.

KWAK, T.A.P. AND TAN, T.H., 1981. The importance of $CaCl_2$ in fluid inclusion trends — evidence from the King Island (Dolphin) skarn deposit. *Econ. Geol. 71*, 955–960.

LEE, A.K., FOO, K.Y. AND ONG, W.S., 1986. Gold mineralisation and prospects in north Pahang Darul Makmur, Peninsular Malaysia. *Geological Survey of Malaysia, Regional Mineral Exploration Report*, 99p.

LEE, A.K., AND CHAND, F., 1981. *Mengapur base metal district, final report on Mengapur Prospect, Phase one diamond drilling.* Unpublished Geological Survey of Malaysia report, No. CB 1/1981, 39p.

LEE, A.K., 1990. Geological and mineral resources of the Hulu Lepar area, Pahang Darul Makmur. *Geological Survey of Malaysia District Memoir 22*, 235p.

MEINERT, L.D., 1993. Igneous petrogenesis and skarn deposits. *In:* Kirkham, R.V., Sinclair, W.D., Thorpe, R.I. and Duke, J.M. (Eds.), *Mineral Deposit Modeling Geol. Assoc. of Canada Special Paper* 40, 565–583.

ROEDDER, E. AND BODNAR, R.J., 1980. Geological pressure determinations from fluid inclusion studies. *Ann Rev Earth Planet Sci 8*, 263-301.

ROEDDER, E., 1984. Fluid inclusions. *In:* Ribbe, P.H. (Ed.), 1984. *Min. Soc. Am. Rev. Mineral. 12*, 644.

SHEPHERD, T.J., RANKIN, A.H. AND ALDERTON, D.H.M., 1985. *A practical guide to fluid inclusion studies*, 1st edn. Blackie, London.

Manuscript received 5 March 2003